IBRACON Structures and Materials Journal
Revista IBRACON de Estruturas e Materiais

ORIGINAL ARTICLE

Localized failure analysis in a large reinforced concrete wall theater

Análise de falha localizada em uma grande parede de concreto armado

Marcos Alves da Silvaᵃ 🄳
Luiz Carlos de Almeidaᵃ 🄳
Leandro Mouta Trautweinᵃ 🄳

ᵃUniversidade Estadual de Campinas – UNICAMP, Departamento de Estruturas, Campinas, São Paulo, Brasil

Abstract: Reinforced concrete structures must be designed in a manner that assures an acceptable level of safety and performance. However, accidents still occur nowadays causing interdiction, financial losses, or even human casualties. Therefore, succinct studies are required to give answers to such an undesirable situation, helping to prevent repetition and enlightening new design and construction methods. This paper analyzes the failure mechanism in a large reinforced concrete panel composed of one L-shaped cantilevered wall and structural walls in Campinas. The investigation was carried out using *in-situ* destructive and non-destructive tests and also through numerical simulation. *In-situ* tests revealed that the region where the fracture happened had no sufficient resisting steel area. The fracture line developed through the end of the wall's horizontal rebars anchored within the column. It was concluded that the reinforced concrete panel failure happened due to structure misconception and incorrect design, once columns stirrups were responsible for the equilibrium of the cantilevered part of the building, as demonstrated by the nonlinear finite element study and *in-situ* investigations.

Keywords: reinforced concrete, numerical analysis, failure mode, structural investigation, *in-situ* tests.

Resumo: Estruturas de concreto armado devem ser projetadas de maneira a garantir um nível aceitável de segurança e desempenho. Porém, acidentes ainda são observados atualmente causando interdições, perdas financeiras, e até mesmo humanas. Portanto, estudos aprofundados são necessários para responder a essas situações indesejáveis, prevenindo sua repetição e desenvolvendo novas formas de dimensionamento e construção. O presente trabalho analisa o mecanismo de falha observado em um extenso painel de concreto armado composto por uma parede em balanço apoiada em um pilar parede, localizados na cidade de Campinas. As investigações foram realizadas *in loco* utilizando testes destrutíveis e não destrutíveis e também via simulações numéricas. Os testes in loco revelaram que a região onde ocorreu a ruptura localizada não possuía quantidade suficiente de armadura metálica. A linha de fratura se desenvolveu no término das armaduras horizontais da parede. Concluiu-se que a falha do painel ocorreu devido a erros de concepção e dimensionamento, dado que os estribos do pilar-parede foram responsáveis pelo equilíbrio da parte em balanço da edificação, como ficou demonstrado pelo estudo utilizando análise não linear via Elementos Finitos e pelas investigações *in-loco*.

Palavras-chave: concreto armado, análise numérica, modo de ruptura, investigação estrutural, testes *in-loco*.

How to cite: M. A. Silva, L. C. Almeida, and L. M. Trautwein, "Localized failure analysis in a large reinforced concrete wall theater" *Rev. IBRACON Estrut. Mater.*, vol. 17, no. 4, e17409, 2024, https://doi.org/10.1590/S1983-41952024000400009

1 INTRODUCTION

Reinforced concrete wall structures are concrete panels that have embedded steel rebars, increasing their tensile strength and overall structural stability. These structural elements are commonly used as vertical and lateral force-

resisting members. The steel rebars in the concrete wall help evenly distribute the stresses and reduce the risk of cracking and collapse. However, like all concrete structures, they are susceptible to pathologies such as the reinforcing steel corrosion, cracking, and spalling of the concrete surface. It is important to use proper design methods, to have good construction control, and maintenance to ensure their long-term durability and performance.

Pathology is the science that studies the origin, mechanisms, symptoms, and nature of diseases. Thus, this science can be understood as the study of the deviation from what is admitted as the normal or expected condition of something, that is, an abnormality that conflicts with the integrity or habitual behavior of the element [1].

In the pathology of constructions, there are several concepts and terms used. One of these terms is the pathological manifestation, which according to Bolina et al. [1] refers to everything that is seen, observed, and presented as indicative of a problem.

Among the numerous pathological manifestations that affect buildings, whether residential, commercial, or institutional, Thomaz [2] reported that the concern of cracks is particularly important, due to three fundamental aspects: the warning of a possible dangerous state for the structure, the performance impairment under service, and the psychological embarrassment that the cracking of the building exerts on users.

Understanding the origin of the pathological manifestation and its causes in a structure is crucial before choosing a correction method. This helps ensure that the chosen rehabilitation or strengthening technique addresses the root of the issue and not just its symptoms.

To this task, numerical simulation through nonlinear finite element analysis (NLFEA) can be used because of its high level of approximation to the real structure behavior, thus analyzing the current stress and strain states. With an NLFEA engineers are allowed to get the structural response under various loads and conditions, and to identify areas of high-stress concentration, poor load distribution, or other factors that may contribute to the development of pathologies. This information can then be used to evaluate the effectiveness of a particular solution for the structural need.

The case study presented in this work has the objective of portraying the partial failure found in a large-scale reinforced concrete building (Figure 1), under construction at the Universidade Estadual de Campinas (UNICAMP), to examine its cause and compose an accurate diagnosis. To detect the pathologies, technical visits were carried out, followed by a detailed study of the structural project, *in-situ* tests, and computational simulations through the Finite Element Method (FEM)
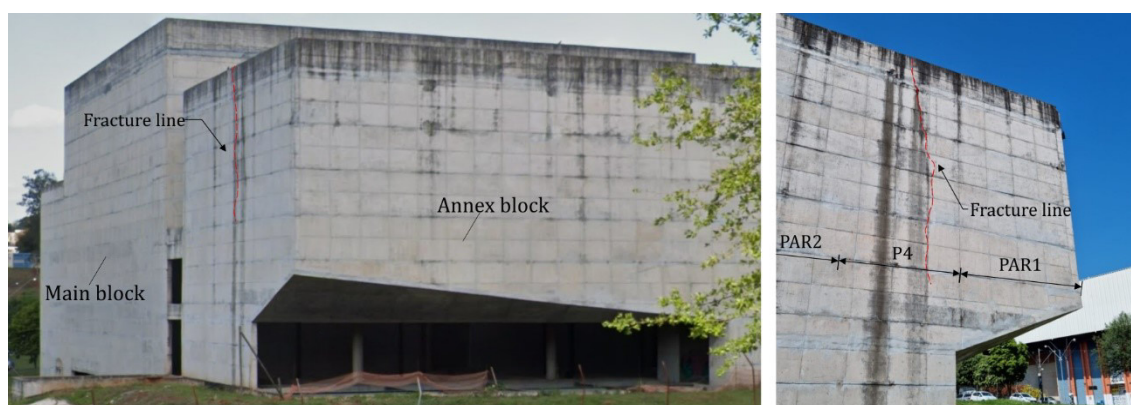

Figure 1. Reinforced concrete building with a localized failure.

2 CASE STUDY

The building, located inside the UNICAMP campus, is an under-construction reinforced concrete building meant to be a theater, comprising two modules: the theater (main block) and the entrance building (annex block) offering access to the theater, made up of three floors, basement, mezzanine, and general top floor, inside a total area of 5669 m^2 (Figure 1).

A technical survey report was carried out on the construction site, due to a localized fracture followed by reinforcement rupture (see Figure 1). Among several pathological manifestations found in the building, this fracture required significant attention because it compromises structural safety. Other pathologies sources were discussed by Almeida et al. [3] and adopted rehabilitation techniques by Silva et al. [4] and Françoso et al. [5].

The rehabilitation project for fractures involves understanding the root of the problem; therefore, the complete survey carried out on-site was aided by an inspection road map. During the visit, a suspicion was raised that the failure

could have been caused by inadequate or missing reinforcement detail, leading to the reinforcement rupture. Afterward, verification of the executive project was performed giving insights into this understanding, jointly with *in-situ* tests.

Figures 2 and 3 reproduce excerpts obtained from the executive project of the structural wall P4 and the cantilever wall PAR1. These elements create a single plane on the annex block front, where the rupture was localized within the P4 boundary. It can be noted in Figure 3a that the P4 structural drawing is a typical column reinforcement detail, with 16mm longitudinal rebars, 6.3mm stirrups and crossties. This could indicate that the designer adopted column elements in the structural model. The PAR1 structural drawing shown in Figure 3b is a typical structural wall reinforcement detail, using a double-layered mesh shape, composed of 8mm vertical and 10mm horizontal steel rebars. However, PAR1 structural drawings presented no information regarding how or if the horizontal rebars should be anchored within the P4. This fact increased the suspicion that the cantilevered-wall equilibrium was being held only by the 6.3mm stirrups. Thus, *in-situ* tests could support this hypothesis by revealing the horizontal anchoring length of PAR1 rebars.
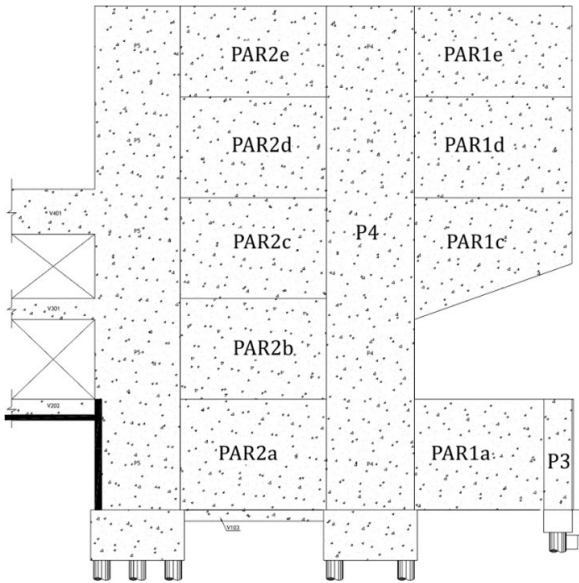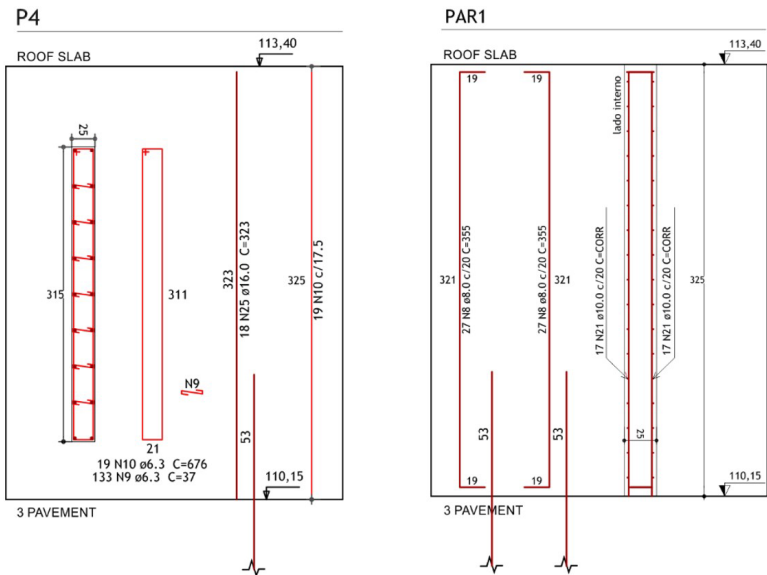

Figure 2. Profile view of the annex block.

(a) Horizontal cross-section view   (b) Profile view

Figure 3. Reinforcement detail of the elements.

2.1 Fracture on P4 structural wall

Different pathologies origins have been identified, arising from construction defects and misconceptions in the structural design [3]. In the photos of Figure 4, both the internal and external faces of the P4 structural wall were presented, where can be observed the extension and opening of the crack. In terms of crack opening, 25 mm in-plane and 28 mm out-of-plane displacements (see Figure 4a) were measured. As a result, some stirrups near the top of the wall ruptured due to the excessive deformation (see Figure 4b).

The photo in Figure 5 shows two cracks in the roof slab along the PAR1 and PAR36, which are perpendicular themselves creating an L-shaped cantilever, together with a concrete detachment. The roof slab cracks were caused by a structural attempt to match displacements between the slab and the supporting walls. The crack appeared on the low-strength connection between slab panels as a consequence of downward and outward movements of PAR1 and PAR36 walls, where the pre-stressed hollow slabs were resting (Figure 5a).

Intersecting walls PAR1 and PAR36 showed a localized concrete detachment as can be observed in Figure 5b. This detachment also resulted from a compatibility attempt equalizing the displacements of walls PAR1 and PAR36 due to the main crack, together with a low reinforcement ratio in this edge.
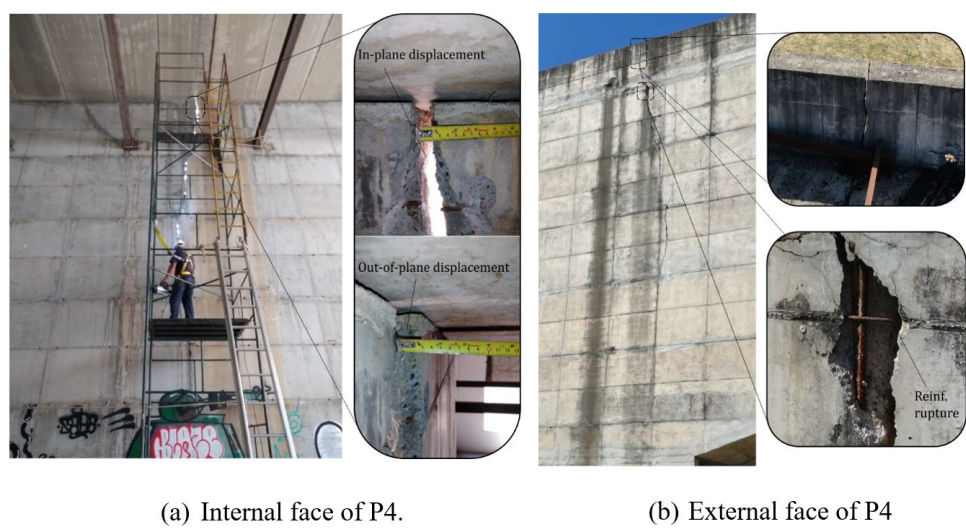

(a) Internal face of P4.   (b) External face of P4

Figure 4. Fracture details on the P4.

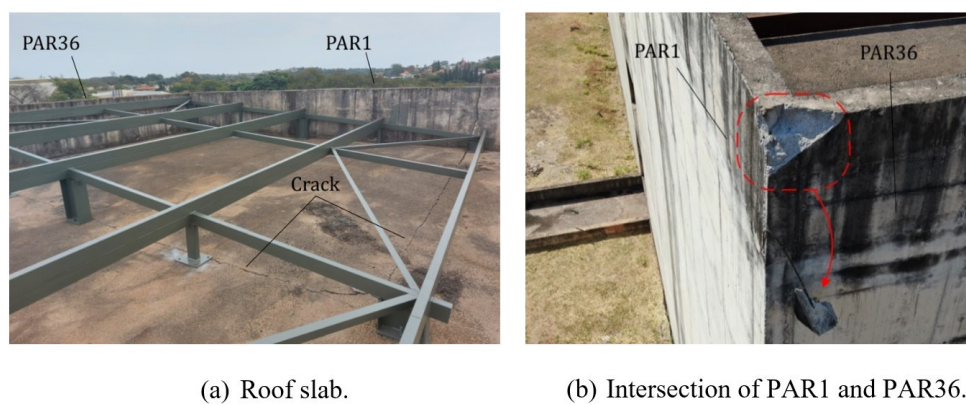(a) Roof slab.   (b) Intersection of PAR1 and PAR36.

Figure 5. Crack pattern of the roof.

2.2 Destructive test

To prove the formulated hypothesis for the reinforcement rupture, that it could have been caused by inadequate or missing reinforcement detail, incisions were made on the inner face of the P4 structural wall next to the crack, as can

be seen in Figure 6. The correct places for the incisions were marked on the wall assisted by a rebar scanner. With these incisions, the P4 reinforcements were identified (stirrups, vertical longitudinal reinforcement, and crosstie), and the PAR01 anchorage length (horizontal longitudinal reinforcement).

The PAR1 horizontal rebars were anchored inside the P4 with diverse lengths. Therefore, the P4 stirrups were indeed supporting the cantilevered part until failure, then the main crack arose. Moreover, the random anchorage pattern explains the appearance of a second crack next to the main crack, pursuing the rebars' tip.

After carrying out the destructive tests, an assembly scheme of the observed *in-situ* reinforcement was created, as illustrated in Figure 7. In the scheme of Figure 7, it can be seen that the PAR1 horizontal reinforcement anchorage length was 60 cm on average. As this part of the structure (PAR01) is analogous to a large deep beam, where the horizontal reinforcements at the top of the wall are those meant to resist the main tensile stresses, the reinforcement detail should have followed this concept. However, the horizontal reinforcement was evenly distributed along the wall instead of being concentrated on the top, at a distance of approximately 15 to 20% of the total height. The Brazilian code ABNT 6118 [6] recommends the steel reinforcement should be distributed within 15% of total height to enlarge the diagonal strut area, thus reducing the compression stress and preventing concrete crushing at the idealized truss node. A strut-and-tie analysis resulted in 24 cm^2 for the steel area on the top while the existing amount is 12.0cm^2. For the strut-and-tie analysis, the support reaction of column P4 was obtained from the numerical model (946kN). The strut compression force was found at the base of P4 considering an inclination of 45°. The traction force on the tie was obtained by the node equilibrium along the upper face of the wall beam. With this traction force, it was possible to estimate the necessary reinforcement for the equilibrium of the model.

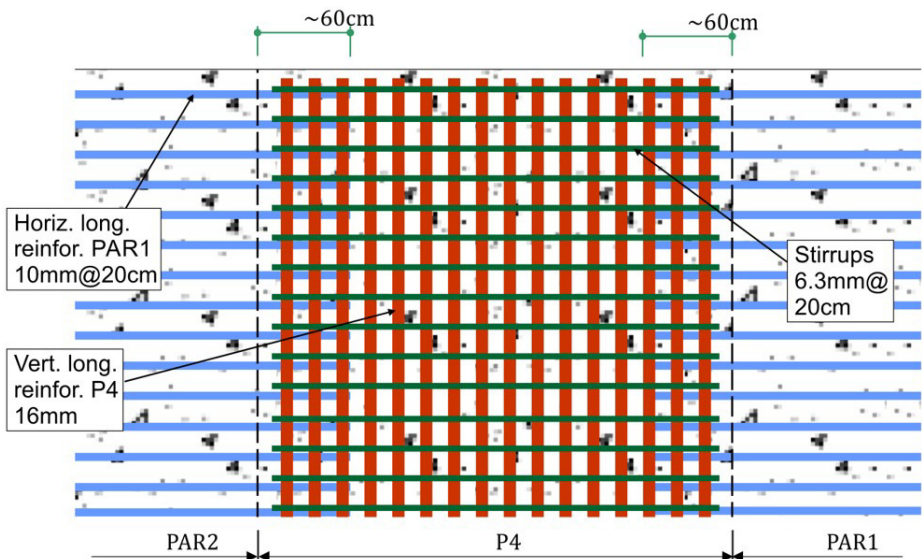**Figure 6.** *In-situ* test.

Figure 7. Reinforcement distribution scheme.

3 NUMERICAL MODEL

A numerical simulation, based on the Finite Element Method (FEM), was performed to comprehend the level of strain the structure was subjected to. For this assignment, the computational software ATENA (v.5) [7] and GiD (v.16) [8], which allow for Non-Linear Finite Element Analysis (NLFEA), were employed to construct and process a localized model from the annex block.

In general, short material properties information is available in executive projects, especially concrete parameters. In the investigated case, only concrete strength (30MPa) and steel yielding (500MPa) were available from structural drawings. The general behavior of concrete and reinforcement constitutive models are depicted in Figure 8 as equivalent uniaxial laws.

3.1 Elements and constitutive models

For the concrete constitutive model (*CC3DNonLinCementitious2*), parameters other than concrete strength are necessary; therefore, main parameters such as tensile strength, Young's Modulus, and fracture energy were obtained according to MC2010 [9]. The cracking model was considered as fixed within the smeared crack formulation; besides, the crack opening was governed by the Hordijk exponential law [10]. To consider possible shrinkage effects on walls a 50% reduction in concrete tensile strength was admitted as recommended by Pryl et al. [11]. The aforementioned constitutive model combines plastic and fracture behaviors, where the compressive plastic behavior is governed by the Menétrey-Willam failure criterion [12] and the fracture behavior is governed by the Rankine criterion. The material parameters employed for the concrete are presented in Table 1. More information regarding the constitutive model can be found in Červenka et al. [7].

For the reinforcement constitutive model (*CCReinforcement*) a bi-linear stress-strain relationship was adopted. The first branch slope (210 GPa) corresponds to the elastic part, then the model assumes perfect plastic behavior. The material parameters employed for the steel reinforcement are presented in Table 2.
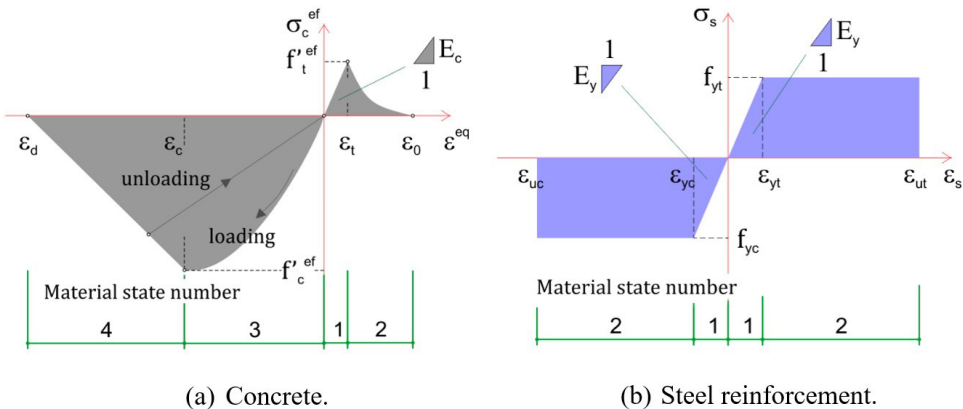

(a) Concrete.   (b) Steel reinforcement.

Figure 8. Uniaxial stress-strain relationship.

The model had 45356 nodes distributed among linear, hexahedral, and prismatic elements. Each linear element used on reinforcements had 2 nodes (*CCIsoTruss* with a linear-shaped function). The hexahedral elements used on walls had 18 nodes (*CCIsoShellBrick* with a quadratic-shaped function). The prismatic elements used for slabs had 12 nodes (*CCIsoShellWedge* with quadratic-shaped function).

An attempt was made to maintain the general aspect ratio 1:1:0.5 (height, width, thickness) for concrete elements to avoid degenerated elements that could compromise the analysis. After performing a three-mesh study using a coarse mesh ($400 \times 400 \times 200 mm^3$), medium mesh ($300 \times 300 \times 200 mm^3$), and fine mesh ($200 \times 200 \times 200 mm^3$), no significant variation was noticed. Thus, the coarse mesh was chosen, except on P4 where a 1:0.5:0.5 aspect ratio was used to better capture the main crack development. The reinforcement elements were considered embedded within concrete elements with a perfect bond assumption.

Table 1. Para meter for the concrete constitutive model.

Parameter	Value	Observation
Compression strength, f_c [MPa]	30	-
On-set of nonlinear behavior, f_{co} [MPa]	4.95	-
Plastic displacement, w_d [mm]	0.5	van Mier [13]
Tension strength, f_t [MPa]	1.18	MC2010 [9] with 50% reduction to consider shrinkage
Fracture energy, G_f [N/m]	135	MC2010 [9]
Crack model	Fixed	-
Young's modulus, E_c [MPa]	31008	MC2010 [9]
Poisson coefficient, ν	0.2	-

Table 2. Parameter for the steel reinforcement constitutive model

Parameter	Value
Yielding stress, f_y [MPa]	500
Young's modulus, E_s [GPa]	210
Ultimate strain, ε_{su} [%]	5

3.2 Boundary conditions

Due to the complex geometry of the building, only part of it was modeled to avoid unnecessary computational work. Therefore, the model comprised a localized region from the annex block represented in Figure 9. The continuity with the remaining parts of the building was simulated by the boundary conditions shown in Figure 9. They restricted the surface translation and rotation movements.

Loading was applied through uniform-distributed pressures along the top of the corbels and cantilevered wall. The loads were estimated by taking into account the type of the roof slab and the supports' influence area.
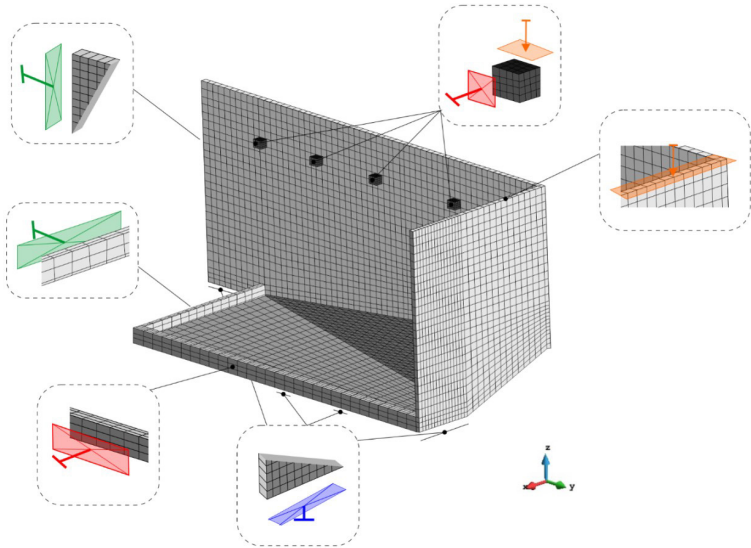

Figure 9. Mesh model and boundary conditions.

A total of three intervals considered the structural elements' construction order. In the first interval, only the self-weight of beams, slabs, walls, and corbels (see Figure 9) were applied. In the second interval, self-weight representing the not-modeled roof slabs was applied to the supporting elements (corbels and walls) as shown in Figure 10. In the third interval, a $25 N/m^2$ load rate distributed along the same influence area of the roof slabs was also applied to the supports. It is worth mentioning that the two initial intervals were divided into 50 load steps whereas, in the final interval, the $25 N/m^2$ load rate representing an overload was applied until failure.

The Newton-Raphson Method, limited to 60 iterations, with a line-search technique was employed to solve the nonlinear problem. Admissible error remained as in default configuration: 1% for displacement and loads (absolute and relative), and 0.01% for energy. When convergence hasn't been achieved, the iteration with the lowest norm error proceeds to the next step. The admitted stop criteria were 10% maximum error between consecutive steps or a sudden load decrease caused by reinforcement yielding.
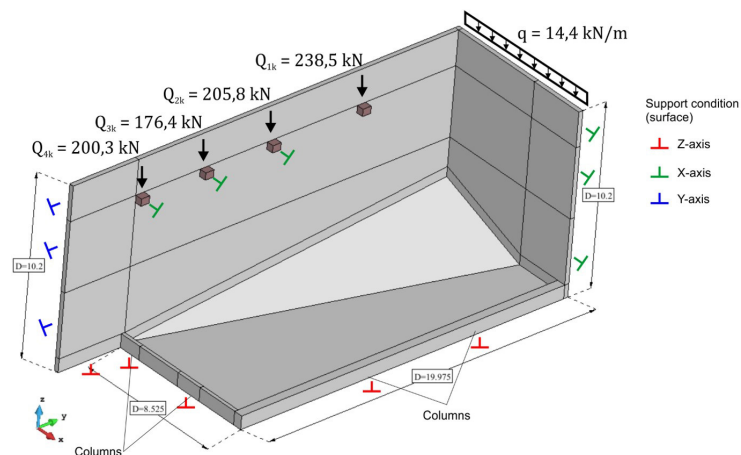
Figure 10. Mesh model and boundary conditions.

4 RESULTS AND DISCUSSION

This section presents obtained results by the NLFEA discussing its similarities with the real building behavior.

Firstly, the summation of vertical loads was checked to validate that the load had been applied properly. In Figure 11 are presented the accumulative vertical reaction from each interval. It can be seen that the self-weight of beams, slabs, walls, and corbels (1st interval) corresponds to 2.588 MN which was checked based on the total volume of concrete ($104m^3$) and the specific weight ($25kN/m^3$). Next, the self-weight from the roof slab (0.953 MN) can be calculated from the 2nd interval and validated when confronted with the roof loads summation (0.944MN) shown in Figure 10. Finally, the overload applied on the roof that caused the failure (0.187 MN) can be calculated from the 3rd interval.

The simulation ended with a 5% overload (0.187 MN). In reality, this load causing the model failure could be explained by accumulated rainwater on the roof due to clogging of the drainage system. Approximately, 35mm of water level is equivalent to 5% overload. Small deviations in walls and slab thicknesses could also justify this 5% overload, especially considering the large areas involved.

Figure 11. Vertical load reaction by interval.

The simulation presented a deformed shape that was compatible with the real structure as can be seen in Figures 12 and 13. It is clear by comparison of the deformed and undeformed shape that the PAR1 wall behaved similarly to a cantilevered member, with a -1.7mm deflection in the model. Besides this vertical displacement, a rotational movement revealed by the slab crack pattern appeared at the top of the intersecting walls, causing an out-of-plane displacement in parts of PAR1 and PAR36. In this situation, PAR1 moved inwards whereas PAR36 moved outwards the building. As a consequence, the fracture line at the wall developed a mixed crack mode (mode I and II) that was also observed *in-situ* (see Figure 4a).

Rev. IBRACON Estrut. Mater., vol. 17, no. 4, e17409, 2024

8/12

The load-displacement curve illustrated in Figure 14 presents the vertical reaction in structural wall P4 versus the vertical displacement in the cantilever end. Upon examination of Figure 15, cracking started through the second interval identified by the stiffness reduction and the large displacement between two consecutive load steps. A single crack advanced vertically within P4 from the top towards its bottom. Afterward, the stiffness was slightly recovered in the third interval due to a stress redistribution, however, it was followed by the stirrup yielding.
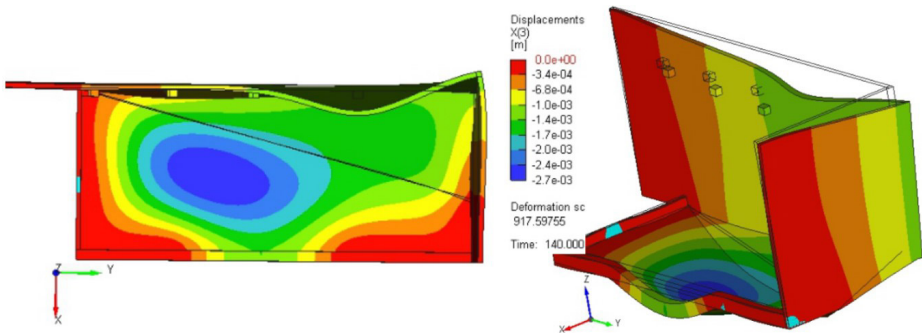

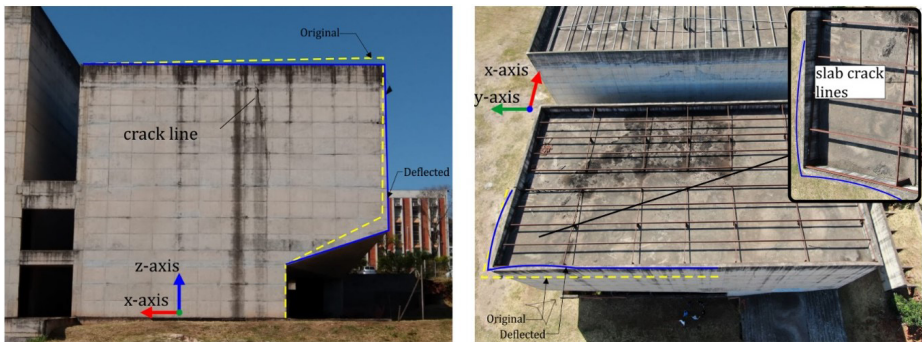**Figure 12.** Deformed shape of the annex block model.

Figure 13. Deformed shape of the annex block.

Cracking evolution in the structural wall P4 is shown in Figure 15. As was described earlier, the horizontal reinforcement of PAR1 and PAR2 was anchored inside P4 (approximately 60cm), thus the fracture line appeared on the borderline of this length. The main crack was initiated at load-step 95 when the P4 vertical reaction was 967 kN, at the end of the roof self-weight loading. When the crack became large enough (0.74mm), several stirrups yielded simultaneously indicating failure.

Figure 16 shows the reinforcement stresses. As can be noted, some horizontal bars were compressed at the bottom, while the rest were tensioned at the top. The cross-section's neutral axis dislocated downwards as the load increased in a typical flexural behavior.
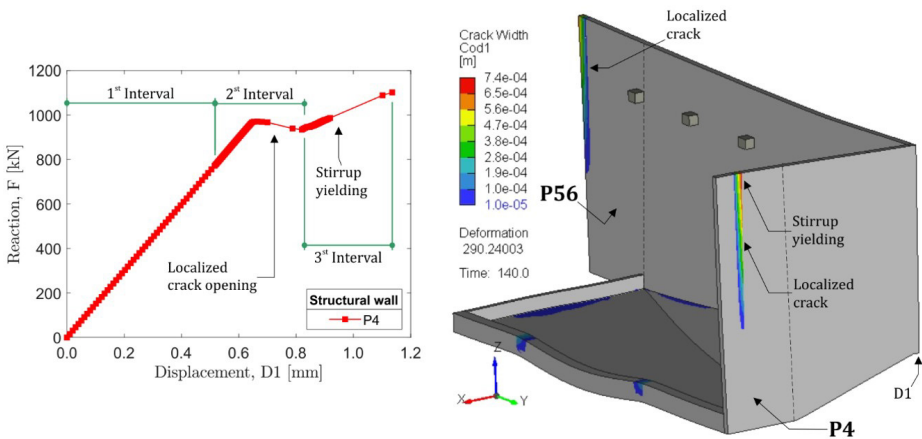

Figure 14. General behavior of the P4 structural wall.

Rev. IBRACON Estrut. Mater., vol. 17, no. 4, e17409, 2024

9/12

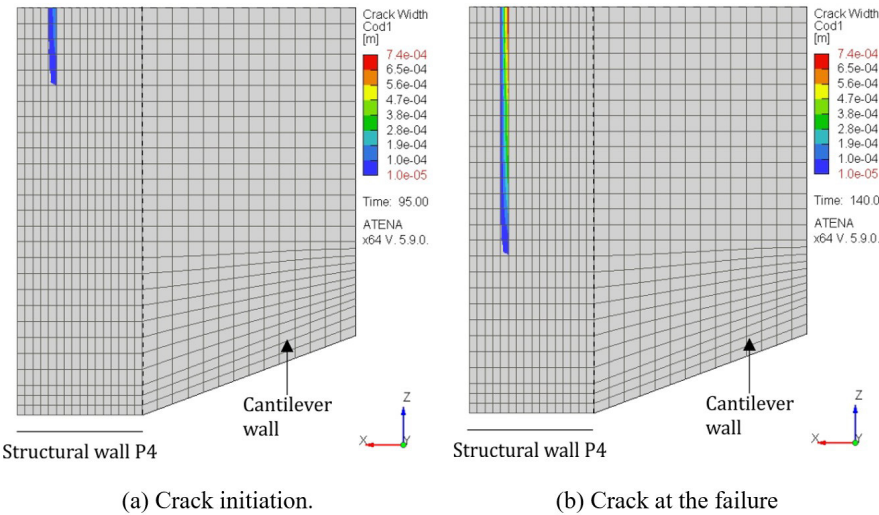(a) Crack initiation.   (b) Crack at the failure

Figure 15. Crack evolution in the P4 structural wall.

It is found in Figure 17 the load-displacement curves of the two structural walls that support the cantilevered part of the building. Four interesting points in this curve explain the failure mechanism that led the P4 stirrups to rupture. As the L-shaped cantilever has two fix two fixed supports (P4 and P56), P4 in the smaller span is the first to yield becoming a semi-elastic support. This change causes stress redistribution with the load migrating to other regions. Nevertheless, the stirrups in P4 remain within the elastic regime providing a resistance reserve. With the load increasing, P56 support at the large span also started to yield changing into a semi-elastic support. Then, the L-shaped cantilever becomes double-hinged and the stirrups strain enters the plastic regime at the P4, leading to rupture.
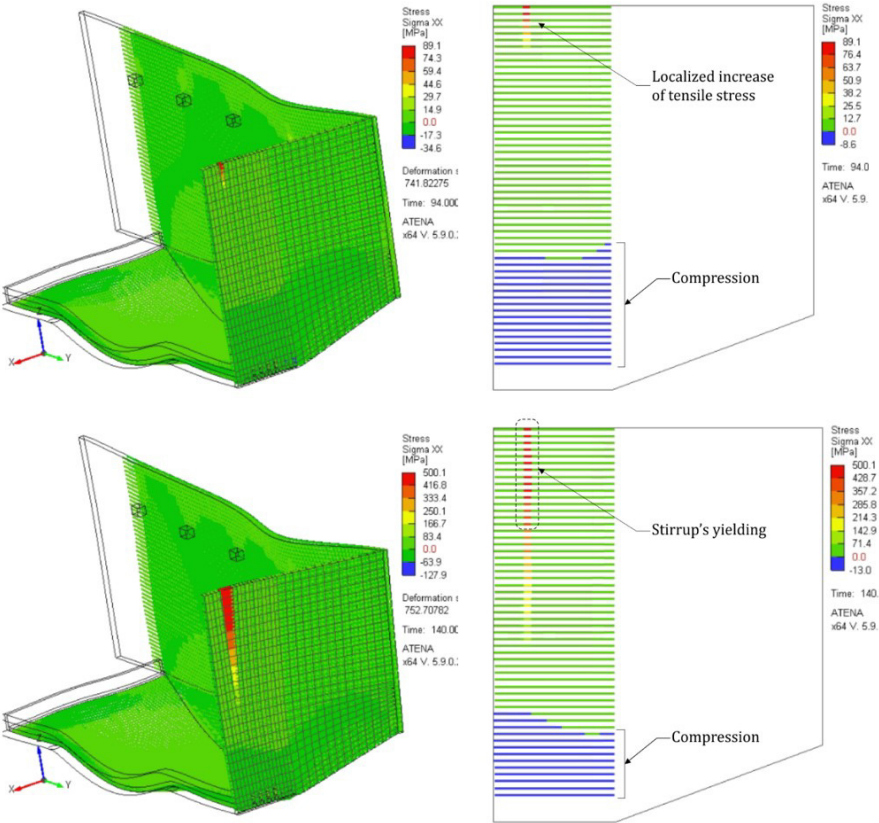

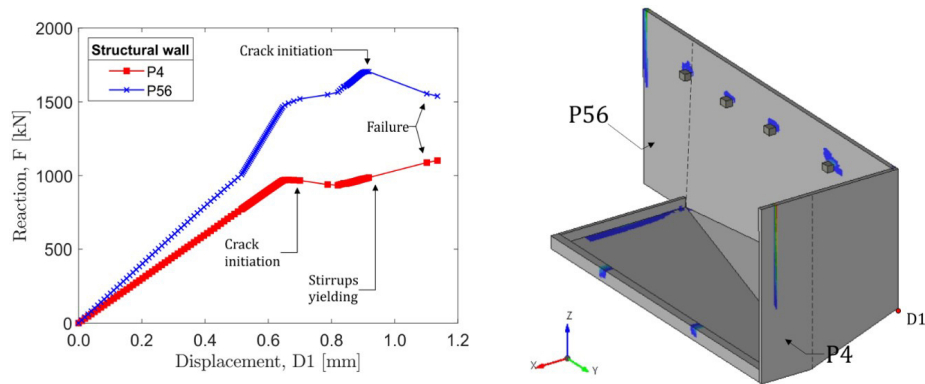**Figure 16.** Reinforcement yielding in the P4 structural wall.

Figure 17. Stiffness pattern of P4 and P56 structural walls.

In Figure 18 are presented the numerical model convergence and reactions in each load step. The forces equilibrium error was the most sensible throughout the analysis with some un-converged steps (error >1%) illustrated in Figure 16a. Most of them are concomitant with the redistribution process caused by the increase of non-linear effects such as cracking, as can be seen in Figure 16b.
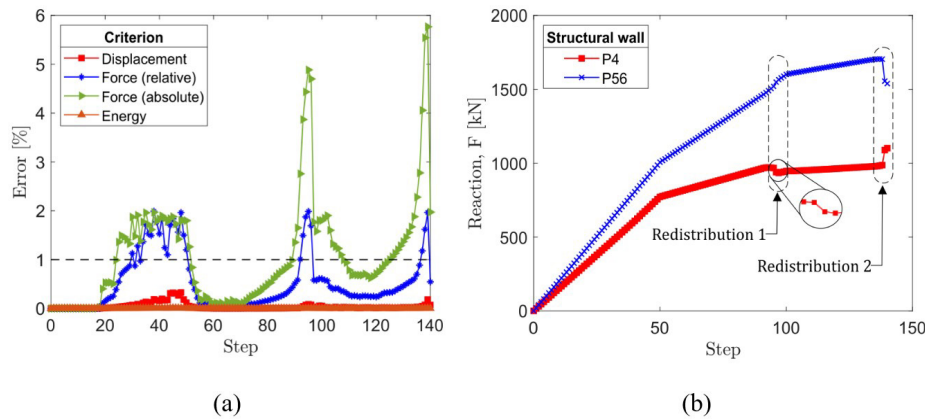

(a)   (b)

Figure 18. Model convergence throughout the loading process.

5 CONCLUSION

Based on the inspections and investigations carried out in the annex block of the building and the NLFEA presented it can be concluded that the structural design significantly compromised the behavior of the P4 and PAR01 walls, highlighting the following points:

- The building structure is composed of RC walls that do not have continuous supports (e.g. continuous footing). However, within these walls, there were regions conceived and detailed as discrete columns (P4, P56, etc.) supported by foundation blocks. There is sufficient evidence that the design method for these "walls" was based on a linear element assumption (bars), and not two-dimensional (plates). With this assumption, the construction presents a complex and mixed behavior between a wall and a column.
- The horizontal PAR1 rebars were anchored at the P4. This decision was probably made by the contractor, once a proper indication of how or if the rebars should be spliced was missing on the structural drawings.
- Due to the continuity's interruption of the walls horizontal, the P4 stirrups were responsible for the cantilever equilibrium. As a result, the amount of steel area provided by the stirrups was not sufficient to withstand the tension stress. A strut-and-tie analysis showed that even if the horizontal rebars were continuously through the P4, the existing steel area would be below the necessary quantity.
- The situation gave rise to a localized and sequential rupture of the P4 stirrups, as the fracture line increased on P4, as demonstrated by the NLFEA and observed on the site.
- The cracks located in the roof slab are consequences of the rupture at P4 and subsequent displacement of PAR01 and PAR36, as shown in the numerical analysis. These displacement compatibility cracks did not cause safety risks to the covering slab.

• Rehabilitation proposals involved the application of carbon-fibers reinforced polymers (CFRP) externally bonded to P4 and PAR1; however, this procedure would require specialized labor to first prepare the structure to then apply the CFPR, in heights up to 10m. Another solution would be to eliminate the free span by including a new column, which seems to be a viable solution despite the architectural impact.

REFERENCES

[1] F. L. Bolina, B. F. Tutikian, and P. Helene, *Patologias das Estruturas*. São Paulo: Oficina de Textos, 2019.

[2] E. Thomaz, *Tricas em Edifícios – Causas, Prevenção e Recuperação*, 2a ed. São Paulo: Oficina de Textos, 2022.

[3] L. C. Almeida, L. M. Trautwein, and C. Basaglia, "Estudo das patologias de projeto e construção em uma estrutura de concreto armado," in *I CBPAT*, Foz do Iguaçu, 2014, pp. 16.

[4] M. A. Silva, A. R. Fanton, L. C. Almeida, L. M. Trautwein, M. Françoso, and I. Marchena, "Different structural monitoring techniques in a large RC building" in *XL CILAMCE*, Natal, 2019, pp. 14.

[5] M. Françoso, I. Marchena, L. C. Almeida, and M. A. Silva, "Precision geometric levelling for the control of vertical displacements in the recovery and reinforcement of a concrete beam, a case study," *Rev. Ing. Constr.*, vol. 34, pp. 205–214, 2019.

[6] Associação Brasileira de Normas Técnicas, *Design of Concrete Structures – Procedure,* ABNT NBR 6118, 2014, 238 p.

[7] V. Červenka, J. Libor, and J. Červenka, "ATENA program documentation, part I, theory," in *ATENA Program Documentation*, Czech Republic, 2020.

[8] A. Coll et al., *GiD v. 16, Reference Manual*. 2018.

[9] International Federation for Structural Concrete, *fib Model Code 2010*, MC2010, 2010.

[10] D. A. Hordijk, "Local approach to fatigue concrete," Ph.D. dissertation, TU Delft, Delft, 1991.

[11] D. Pryl, J. Libor, and J. Červenka, "ATENA program documentation, part XI, troubleshooting manual" in *ATENA Program Documentation*, Czech Republic, 2020.

[12] P. Menétrey and K. Willam, "Triaxial failure criterion for concrete and its generalization," *ACI Struct. J.*, vol. 92, no. 3, pp. 311–318, 1995.

[13] J. G. M. van Mier, "Multiaxial strain-softening of concrete," *Mater. Struct.*, vol. 19, no. 3, pp. 179–190, 1986.

Author contributions: MAS: investigation, data curation, writing – original draft; LCA: supervision, project administration, funding acquisition, writing - review & editing; LMT: supervision, project administration, funding acquisition, writing - review & editing.

Editors: Bernardo Horowitz, Guilherme Aris Parsekian.